Accelerating beam propagation in refractive-index potentials

Nikolaos K. Efremidis*
Department of Applied Mathematics, University of Crete, 71409 Heraklion, Crete, Greece
(Received 22 December 2013; published 25 February 2014)

We study the dynamics of spatially accelerating beams impinging on refractive-index potentials. We concentrate our attention to the particular case of Airy-type optical waves that are reflected and transmitted by two generic classes of potentials. These are (a) localized potentials whose index contrast reduces to zero outside a specific region and (b) smooth-interface sigmoid-type potentials that take different constant values outside a bounded region. We find analytic expressions for the beam dynamics for particular types of potentials which are in excellent agreement with the numerical simulations. Our results show that, in general, the parabolic trajectory of the Airy wave is not maintained by the transmitted and reflected waves. An exception is made in the case of reflection from piecewise linear potentials, where the reflected wave follows a parabolic trajectory that is, in general, different from the incident.

DOI: 10.1103/PhysRevA.89.023841 PACS number(s): 42.25.Fx, 42.15.Dp, 42.25.Gy

I. INTRODUCTION

The study of curved and accelerated waves has attracted a lot of attention over the past years [1]. This interest was first triggered by the theoretical [2] and experimental [3] study on Airy beams, where it was demonstrated that exponentially truncated Airy beams can be constructed by applying a Fourier transform to a Gaussian beam with a cubic phase. Within the context of quantum mechanics, the Airy wave was first found to be a solution of the potential free Schrödinger equation [4]. The Airy function can be considered as a basic prototype in catastrophe theory that describes the fold-type catastrophe [5]. It is worth pointing out that the Airy wave is the only diffraction-free localized solution of the $1+1$-dimensional ($1+1$D) Schrödinger equation. Furthermore, its trajectory bends and follows a parabola. Curved beams are not limited to following parabolic trajectories but can also follow arbitrary convex trajectories, by "sacrificing" their diffraction-free properties [6–8].

Since 2007, several different configurations and applications have been found for such curved beams. These include filamentation [9], particle manipulation [10,11], micromachining [12], and Airy plasmons [13–15]. In higher dimensions paraxial accelerating beams have also been studied. In particular $2+1$D curved diffraction-free beams can exist as superposition of Airy waves [2,3] or in the form of parabolic beams [16]. Abruptly autofocusing waves are radially symmetric Airy beams whose maximum intensity profile exhibits an abrupt peak at the focus [17]. Such beams have been utilized for ablation [18], particle manipulation [11], and filamentation [19]. Spatiotemporal curved beams have been contracted in the form of optical light bullets [20]. Nonparaxial configurations have also been studied and have the advantage that the transverse acceleration of the beams can be significantly increased [21–23]. In addition, light can follow curved trajectories in periodic array configurations by utilizing the Floquet structure of the system [24–27]. Besides optics, curved and accelerated waves have been considered in different settings such as in electron beams [28], in matter waves [29], and in antenna arrays [30].

Up to now most of the studies on Airy wave have been limited to uniform media. Considering nonuniform index configurations it is known that when an Airy wave propagates in a medium with a transversely linear index gradient (x direction) which varies with the propagation distance z [i.e., $V = xf(z)$], then the dyanamics are exact solvable. Specifically, the Airy wave can follow trajectories that are different from the parabolic, depending on the particular choice of $f(z)$ [4,31]. Furthermore, and in connection to this study, reflection and refraction of Airy beams at the interface between two dielectric media was investigated in [32]. The nonlinear problem was also studied numerically by solving the nonlinear Helmholtz equation [33]. However, in these works [32,33] the study is limited to abrupt interfaces between two different media.

In this paper, we study the scattering problem of an Airy beam impinging on refractive index potentials. In particular, we investigate two different generic classes of potentials, which are (a) spatially localized potentials whose index contrast goes to zero outside a bounded region and (b) sigmoid potentials that have different constant indices outside an intermediate region where the index changes smoothly. We show that in contrast to the case of abrupt dielectric interfaces [32], where the reflected and refracted waves have the same structure as the incident Airy wave, for smoothly varying potentials the dynamics are more complicated. In particular, we find that, in general, both the reflected and refracted beams do not follow parabolic trajectories and thus do not have the functional form of an Airy wave. An exception is the case of a piecewise linear potential where the reflected beam maintains the structure of the Airy wave but with reduced acceleration (and thus larger width). Interestingly enough, in this latter case the trajectory of the reflected Airy wave can be controlled by tuning the index gradient.

II. CURVED BEAMS IMPINGING ON INDEX POTENTIALS

We start our analysis by using a differential approach based on the normalized paraxial equation,

$$i\psi_z + (1/2)\psi_{xx} - V(x,z)\psi = 0, \tag{1}$$

*nefrem@tem.uoc.gr

where ψ is the amplitude of the optical wave, x is the transverse and z is the propagation coordinate, and the potential $V(x,z)$ is inversely proportional to the refractive-index modulations. In addition, we define as ξ the transverse spatial coordinate x at the input plane $z=0$. We decompose the optical wave into amplitude and phase $\psi=\rho^{1/2}e^{i\phi}$ leading to

$$\frac{\partial\rho}{\partial z}+\frac{\partial(\rho u)}{\partial x}=0,\quad \frac{\partial u}{\partial z}+u\frac{\partial u}{\partial x}=-\frac{\partial V}{\partial x}, \tag{2}$$

where $u=\phi_x$, and we have ignored the so-called "quantum pressure term" $(\partial_x[(2\rho_{xx}\rho-\rho_x^2)/(8\rho^2)])$ from the right-hand side of the second part of Eqs. (2) that accounts for diffraction. Thus Eqs. (2) provide the ray optics approximation of the paraxial equation. If the potential is z invariant, then the second part in Eqs. (2) can be reduced to $dx/dz=u$ along with the conservation law

$$E(\xi)=V(x)+\frac{u^2}{2} \tag{3}$$

that can be considered as the sum of the "potential energy" $V(x)$ and "kinetic energy" $u^2/2$. Equation (3) represents the conservation of the momentum along the propagation coordinate. In addition, the first part of Eqs. (2) (conservation of power) reduces to $d_z\rho=-\rho\partial_x u$.

We can utilize different, but equivalent, approaches to obtain the beam trajectories. For example, by taking the partial derivative of the second part of Eqs. (2) with respect to x we obtain a Riccati type equation for $u_x(x(z),z)$ which can be linearized via $u_x(x(z),z)=g'(z)/g(z)$ to give $g''+V_{xx}(x(z),z)g=0$. Solving for initial conditions that satisfy $g'(0;\xi)=g(0;\xi)u_x(\xi)$ we can determine the caustic distance $z_c(\xi)$ from the requirement $g(z_c,\xi)=0$. Interestingly enough for a medium with a linear transverse index modulation, i.e., $V(x,z)=xG(z)$, we have that $V_{xx}=0$ and thus the caustic distance z_c remains unaffected by the presence of the potential. Such a potential can be eliminated from the paraxial equation via a simple transformation. Thus solutions of the potential-free paraxial equations are mapped into solutions of the paraxial equation with a z-dependent linear index potential. This mapping in the case of the Airy function has been discussed in the literature [4,31]. An alternative method for the derivation of the caustics is to utilize the implicit function theorem and set $F_\xi(x,z,\xi)=0$, where $F(x,z,\xi)=0$ represents the ray equation.

The dynamics of rays and caustics in the presence of potentials can be derived by integrating $dx/dz=u$ using the conservation law of Eq. (3) that leads to

$$z=\int_\xi^x\frac{dx}{u(x;\xi)}, \tag{4}$$

where $u(x;\xi)=\sqrt{2[E(\xi)-V(x)]}$ is the transverse spatial velocity of the ray and ξ is the initial transverse coordinate. In the case of reflection, we can determine the transverse coordinate where each ray is going to get reflected $x_r(\xi)$ by solving the algebraic equation

$$E(\xi)=V(x_r).$$

The dynamics of the reflected rays are then given by

$$z=\int_\xi^{x_r}\frac{dx}{u(x)}+\int_x^{x_r}\frac{dx}{u(x)},\quad x<x_r. \tag{5}$$

The case of a curved beam propagating in a homogeneous medium has been well examined [6–8]. Specifically, for a power-law input phase,

$$\phi(z=0)=-\frac{(-\gamma\xi)^b}{\gamma b}, \tag{6}$$

we have that $u(z=0)=(-\gamma\xi)^{b-1}$ for $\xi<0$ where, for a power-law trajectory, $1<b<2$. Substituting Eq. (6) to Eq. (4) and after some algebraic calculations, we can derive the beam trajectory

$$x_c=(2-b)[\gamma(b-1)]^{\frac{b-1}{2-b}}z_c^{\frac{1}{2-b}}, \tag{7}$$

where, for clarity, we use the notation x_c,z_c for the caustic coordinates. When $b=3/2$ the resulting solution takes the form of the Airy beam [2], which is the only localized diffraction-free solution of the paraxial equation in one dimension. The trajectory of the Airy beam is parabolic $x=\gamma(z/2)^2$ and its amplitude profile decays as $\rho^{1/2}\sim(-\xi)^{-1/2}$.

III. LOCALIZED POTENTIALS

In this section, we are going to consider the dynamics of Airy beams impinging on transversely localized, z-invariant potentials such that $V(x)=0$ as $x\to\pm\infty$. Without loss of generality, we assume that the beam initially moves from the left to the right. We can distinguish two different cases according to which (1) the ray has enough transverse momentum to be transmitted $E>\max V$ and (2) the ray gets reflected by the potential $0<E<\max V$.

For the transmitted rays we can directly integrate Eq. (4) for all $z>0$. Furthermore, assuming that the potential is compact [$V(x)=0$ outside some bounded region $x_1<x<x_2$] or that $V(x)$ is small enough and fast decaying outside (x_1,x_2), then we can quantify the effect of the potential to the beam trajectory for $x>x_2$. In particular, for $x<x_1$ the ray equation is $x=\xi+u_0(\xi)z$ [where we define $u_0(\xi)=u(\xi,z=0)$], whereas for $x>x_2$ we obtain

$$x=\xi+F(\xi)+u_0(\xi)z, \tag{8}$$

where

$$F[E(\xi);V]=\int_{-\infty}^{\infty}\left[1-\frac{u_0(\xi)}{u(x;\xi)}\right]dx. \tag{9}$$

In the above integral we have extended the limits of integration to the real line. We see that F is a function of $E(\xi)$ but is also a functional of the index potential $V(x)$. We also note that the transverse spatial velocity of each ray outside the potential is the same. Thus before and after the potential each ray is parallel to itself and is shifted by $F(\xi)$. Specifically, if the potential $V(x)$ is positive (the index contrast is negative) the velocity of the ray $u(x;\xi)$ decreases as it passes through the potential and thus F is negative. On the other hand, if $V(x)\leqslant 0$ then $F\geqslant 0$. An alternative form for the transmitted ray trajectories is

$$x=x_2+u_0(\xi)[z-z_2(\xi)],\quad z>z_2(z), \tag{10}$$

where $z_2 = (x_2 - \xi)/u_0(\xi) - F/u_0(\xi)$ is the sum of the propagation length required for the ray to move from ξ to x_2 with transverse spatial velocity $u_0(\xi)$ plus the difference in the propagation length due to the potential. As a consequence of the potential mediated ray shifting the trajectory of the transmitted beam is going to be modified as compared to the case without potential. The general expression for the beam trajectory for $x > x_2$ is then given by

$$z_c = -\frac{F'(\xi)+1}{u_0'(\xi)}, \quad x_c = \xi + F(\xi) - \frac{u_0(\xi)[1+F'(\xi)]}{u_0'(\xi)}, \tag{11}$$

where, for an Airy incident, $u_0/u_0' = 2\xi$.

The trajectory of the reflected rays can be determined by integrating Eq. (5). In particular, we have

$$x = 2x_1 - \xi + F(\xi) - u_0(\xi)z,$$

where

$$F[\xi; V] = \int_{x_1}^{x_r(\xi)} \frac{2u_0(\xi)dx}{u(x;\xi)}.$$

We can also write the above equation as

$$x = x_1 - u_0(\xi)[z - z_2(\xi)], \quad z > z_2(\xi),$$

where

$$z_2(\xi) = \frac{x_1 - \xi}{u_0(\xi)} + \frac{F(\xi)}{u_0(\xi)}$$

is the propagation length required for the beam to go from ξ to x_r, and reflect back to x_1.

We are now going to consider the particular case of the following squared hyperbolic secant potential:

$$V(x) = \alpha \ \mathrm{sech}^2 \frac{x - x_0}{\beta}, \tag{12}$$

which is centered at $x = x_0$, has amplitude α, and width proportional to β. For convenience we introduce the transverse coordinates

$$y = (x - x_0)/\beta, \quad \eta = (\xi - x_0)/\beta. \tag{13}$$

By direct integration we find that the rays that get transmitted satisfy

$$y = \mathrm{arcsinh}\left\{A \ \sinh\left[\mathrm{arcsinh}\frac{\sinh\eta}{A} + \frac{\sqrt{2E(\xi)}z}{\beta}\right]\right\}, \tag{14}$$

where the above equation holds for all $z > 0$, and

$$A(\xi) = \left(1 - \frac{\alpha}{E(\xi)}\right)^{1/2}. \tag{15}$$

For Airy waves and assuming that the index contrast is almost zero at the initial transverse coordinate ξ we have that $E(\xi) = -\gamma\xi/2$. Furthermore, from Eq. (9) we can find that $F[E(\xi); V] = 2\beta \log A$, where log denotes the natural logarithm. Thus for $x > x_2 \approx x_0 + 2\beta$ and $z > z_2 \approx (x_2 - \xi)/\sqrt{2E(\xi)} - 2\beta \log A/\sqrt{2E(\xi)}$, we can simplify Eq. (14) to take the form

$$x = \xi + \sqrt{2E(\xi)}z + 2\beta \log A. \tag{16}$$

The transmitted beam trajectory can be computed analytically from Eq. (14); however, the full expressions are rather complicated and we prefer not to present them. Instead, the caustic formulas are significantly simplified for the transmitted rays $z \gtrsim z_2$, in which case we can utilize the asymptotic ray Eq. (16) to find

$$z_c = 2\sqrt{\frac{-\xi}{\gamma}}\left(1 - \frac{2\alpha\beta}{\xi(\gamma\xi + 2\alpha)}\right), \tag{17}$$

along with

$$x_c = -\xi + \frac{4\alpha\beta}{\gamma\xi + 2\alpha} + \beta \log\left(1 + \frac{2\alpha}{\gamma\xi}\right). \tag{18}$$

In Eqs. (17) and (18), the first terms on the right-hand side describe the Airy beam trajectory, while the remaining terms are due to the distortion caused by the hyperbolic secant potential. Thus the transmitted beam trajectory is not parabolic and cannot be described by an Airy function. We note that in Eqs. (17) and (18) the parabolic trajectory is recovered only if the conditions $E(\xi) \gg \alpha$ and $E(\xi) \gg \sqrt{\alpha\beta/\gamma}$ are satisfied. However, this is a trivial reduction that describes the case where the potential is weak as compared to the transverse momentum of the ray.

Rays that do not have enough transverse momentum [$\alpha > E(\xi)$] are reflected by the potential. Integrating Eq. (4) we find that before the reflection ($z < z_r$) the ray equation satisfies

$$y = -\mathrm{arcsinh}\left\{A \ \cosh\left[\mathrm{arccosh}\frac{-\sinh\eta}{A} - \frac{\sqrt{2E(\xi)}z}{\beta}\right]\right\}, \tag{19}$$

where

$$A(\xi) = \left(\frac{\alpha}{E(\xi)} - 1\right)^{1/2}, \tag{20}$$

and the reflection coordinates are given by

$$y_r = -\mathrm{arcsinh}A, \tag{21}$$

$$z_r = \frac{\beta}{\sqrt{2E(\xi)}}\mathrm{arccosh}\frac{-\sinh\eta}{A}. \tag{22}$$

Furthermore, the reflected rays ($z > z_r$) satisfy

$$y = -\mathrm{arcsinh}\left\{A \ \cosh\left[\frac{\sqrt{2E(\xi)}(z - z_r)}{\beta}\right]\right\}. \tag{23}$$

In Fig. 1 we see typical dynamics of an Airy beam impinging on a squared hyperbolic secant potential as given by Eq. (12). We note that all our numerical simulations on Eq. (1) were performed using a fourth-order split-step Fourier method for the diffraction and the potential terms. In Figs. 1(a) and 1(b) the potential is negative ($\alpha < 0$) meaning that the index is increased towards the center of the potential. As a result the rays and the beam trajectory accelerate as they approach the center of the potential and then they decelerate to recover their initial velocity. Thus the beam trajectory is shifted to the right as compared to the potential-free dynamics of an Airy beam. In Figs. 1(c) and 1(d) the refractive index decreases towards the

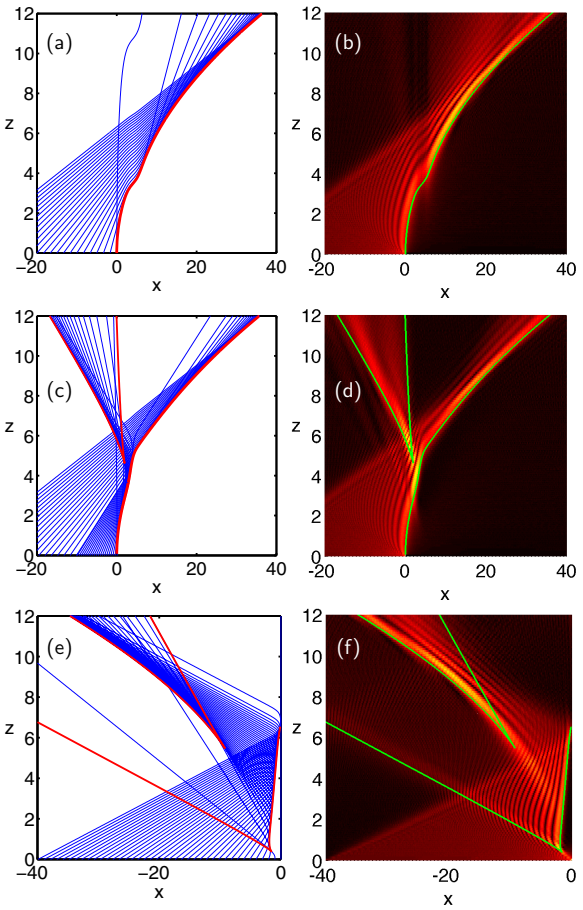

FIG. 1. (Color online) Dynamics of Airy beams impinging to a squared hyperbolic secant index profile given by Eq. (12). On the left we see the asymptotic ray dynamics (blue lines) and the caustic trajectories (thick red lines). On the right we see the corresponding direct simulations and the caustic lines in green. The parameters are as follows: in the top row $\alpha = -8$, $\beta = 1$, and $x_0 = 4$, in the middle row $\alpha = 5$, $\beta = 1$, and $x_0 = 4$, and in the bottom row $\alpha = 20$, $\beta = 1$, and $x_0 = 0$.

center of the potential ($\alpha > 0$). Thus the rays decelerate as they approach the index minimum, and only those that have enough transverse momentum will get transmitted. The trajectory of the transmitted beam (fold caustic) is shifted to the left as compared to the potential-free Airy beam trajectory, consists of both transmitted and reflected rays, and is given by Eqs. (17) and (18) for $x > x_2$. The reflected rays form an additional caustic which is of the cusp type. It is interesting to point out that the same rays that get reflected contribute to both the fold and the cusp caustics. In Figs. 1(e) and 1(f) we have chosen the potential height α and the extent of the Airy beam such that the whole beam gets reflected. The caustic structure reveals the creation of a second cusp (the lower one), as compared to Figs. 1(c) and 1(d). The left branch of the lower cusp is generated from rays that are reflected before they form a caustic.

We have also tested different types of potentials with similar results. For example, we can create a localized potential by using piecewise linear functions. The reflection properties of these potentials are identical to those discussed in the next section. The transmitted beam also gets deformed as compared to the incident parabolic trajectory.

IV. SIGMOID POTENTIALS

The second class of potential that we are going to analyze has the form of sigmoid functions (functions that take different constant values as $x \to \pm\infty$ and in between they have a smooth enough and monotonic profile). It is instructive to consider such a generic potential $V(x)$ which is constant outside (x_1,x_2) with $V(x) = V_1$ for $x < x_1$ and $V(x) = V_2$ for $x > x_2$. In between we can assume that $V(x)$ is a continuous and monotonic function that connects the two states. From the conservation law given by Eq. (3) we find that the transmitted wave has spatial velocity

$$u_2(\xi) = \sqrt{u_0^2(\xi) + 2(V_1 - V_2)}, \quad x > x_2.$$

By integration of Eq. (4) we obtain the ray equation

$$x = x_2 - \frac{u_2(\xi)}{u_0(\xi)}(x_2 - \xi) + F(\xi; V) + u_2(\xi)z, \tag{24}$$

where

$$F[\xi; V] = \int_{x_1}^{x_2} \frac{u_2(\xi)[u(x;\xi) - u_0(\xi)]}{u_0(\xi)u(x;\xi)}dx.$$

Note that we can also write Eq. (24) in the form

$$x = x_2 + u_2(\xi)[z - z_2(\xi)],$$

where

$$z_2(\xi) = \frac{x_2 - \xi}{u_0(\xi)} - \frac{F(\xi; V)}{u_2(\xi)}.$$

The transmitted beam trajectory (for $z > z_2$) is then given by

$$z_c = z_2 + \frac{u_2 z_2'}{u_2'}, \quad x_c = x_2 + \frac{u_2^2 z_2'}{u_2'}.$$

In many relevant cases the potential does not become exactly V_1 and V_2 outside a bounded region (x_1,x_2) but asymptotically reaches these values at $\pm\infty$. In these cases, we can still utilize the above expressions by choosing approximate values for x_1 and x_2 and modifying the functional form F to

$$F = \int_{-\infty}^{\infty} \left(\frac{u_2(\xi)}{u(x;\xi)} - \frac{H(x_2 - x)u_2(\xi)}{u_0(\xi)} - H(x - x_2) \right) dx.$$

On the other hand, for the reflected rays we can follow the exact same analysis as in previous section.

Let us now consider the particular example of a piecewise linear potential of the form

$$V(x) = \begin{cases} -\alpha, & x - x_0 < -\beta, \\ \alpha(x - x_0)/\beta, & -\beta < x - x_0 < \beta, \\ \alpha, & x - x_0 > \beta, \end{cases} \tag{25}$$

where $2\beta > 0$ is the extent of the potential, α is the potential contrast, and x_0 is the center of the potential. Using the normalized coordinates of Eqs. (13) we can express the

potential as

$$V(y) = \begin{cases} -\alpha, & y < -1, \\ \alpha y, & -1 < y < 1, \\ \alpha, & y > 1. \end{cases}$$

Up to $y = -1$ (or $x = x_1 = x_0 - \beta$) the rays are not affected by the presence of the potential and thus $y = \eta + \sqrt{-\gamma\xi}z/\beta$. Setting $y = -1$, we find that the aforementioned equations hold up to $z = z_1$, where

$$z_1 = (x_0 - \xi - \beta)/\sqrt{-\gamma\xi}. \tag{26}$$

At $z = z_1$ the rays enter the area with the linear index gradient that is causing a parabolic bending of the rays,

$$y = \frac{x - x_0}{\beta} = -1 + \frac{\sqrt{-\gamma\xi}(z - z_1)}{\beta} - \frac{\alpha(z - z_1)^2}{2\beta^2}. \tag{27}$$

At this point we have to distinguish two different scenarios depending on the initial transverse momentum of the ray. In particular, if the transverse momentum is large enough [$E(\xi) > V(\infty)$ or $-\gamma\xi - 4\alpha > 0$] the rays get transmitted. Thus Eq. (27) holds up to $y = 1$ and $z = z_2$, where

$$z_2 = z_1 + \frac{\beta}{\alpha}[\sqrt{-\gamma\xi} - \sqrt{-\gamma\xi - 4\alpha}]. \tag{28}$$

Finally, for $z > z_2$ the ray equation becomes linear again,

$$y = 1 + \frac{\sqrt{-\gamma\xi - 4\alpha}(z - z_2)}{\beta}. \tag{29}$$

On the other hand, if the rays do not have enough momentum to get transmitted through the potential, then they follow a parabolic trajectory and eventually they return to $y = -1$ at

$$z_2 = z_1 + \frac{2\beta\sqrt{-\gamma\xi}}{\alpha}.$$

For $z > z_2$ the ray equation is given by

$$y = -1 - \frac{\sqrt{-\gamma\xi}(z - z_2)}{\beta}. \tag{30}$$

The next step is to determine the beam trajectory of an incident Airy-type wave. For $z < z_1$ the beam trajectory is parabolic with $x_c = \gamma z_c^2/4$. Then, inside the constant index gradient medium ($-1 < y < 1$ and $z_1 < z < z_2$) its trajectory $[x_c(\xi), z_c(\xi)]$ is determined by the equations

$$z_c = \frac{\alpha x_1^2 - \xi^2(\alpha + 2\beta\gamma)}{\sqrt{-\gamma\xi}[\alpha(\xi + x_1) + \beta\gamma\xi]}, \tag{31}$$

$$x_c = \frac{\beta\gamma\xi\left[2\alpha\left(x_1^2 - \xi^2\right) - 2\beta\gamma\xi^2\right] + \alpha(\xi + x_1)^2(\beta\gamma\xi + 2\alpha x_1)}{2[\alpha(\xi + x_1) + \beta\gamma\xi]^2}. \tag{32}$$

For the rays that get transmitted $y > 1$ (and $z > z_2$), we have that

$$z_c = \frac{2\{2\alpha^2(x_1 + \xi) + \alpha\gamma\xi^2 + \beta\gamma\xi[\sqrt{\gamma\xi(4\alpha + \gamma\xi)} + \gamma\xi + 2\alpha]\}}{\alpha(-\gamma\xi)^{3/2}}, \tag{33}$$

$$x_c = 5\beta + x_0 + \frac{\beta\gamma\xi}{\alpha} - \left(\frac{4\alpha + \gamma\xi}{\gamma\xi}\right)^{3/2}\frac{\alpha(\xi + x_1) + \beta\gamma\xi}{\alpha}. \tag{34}$$

Finally, for the reflected rays ($y < -1$ and $z > z_2$) the beam trajectory is explicitly given by

$$x_c = 2(x_0 - \beta) - \frac{\alpha\gamma z_c^2}{4(\alpha + 2\beta\gamma)}. \tag{35}$$

It is interesting to point out that the reflected beam maintains the form of an Airy wave, since its trajectory is parabolic. The direction of the Airy beam is the opposite from the incident, and it is shifted by $2(x_0 - \beta)$. Furthermore, the coefficient of the parabolic term differs from the incident one by a factor of $\sigma = 1/[1 + (2\beta\gamma/\alpha)]$ such that $0 < \sigma < 1$ ($\alpha, \beta, \gamma > 0$). Thus an incident Airy wave through reflection is transformed to another Airy wave which is slower and wider [the width of the reflected Airy wave is given by $1/(\gamma\sigma)^{1/3}$]. By inspection of σ, we see that for a steep enough potential $\alpha \gg 2\beta\gamma$ the reflected Airy wave becomes identical to the incident. This limiting case is in agreement with [32] where the interface dynamics of Airy beams were studied. In the other limit case where the index gradient is relatively small $2\beta\gamma \gg \alpha$, the coefficient of the parabolic term of the trajectory becomes $\alpha/(8\beta)$ and is independent of γ. Thus, for the same potential, the reflected Airy beam will be almost identical independent of the width of the incident Airy beam as long as the above inequality holds.

In Fig. 2 we show typical dynamics of an Airy wave impinging on a piecewise linear sigmoid potential. In particular, in Figs. 2(a) and 2(b), $\alpha > 0$ and thus the rays that do not have enough momentum are going to be reflected. We note the generation of a fold "transmitted" beam as well as a cusp caustic. The reflected rays contribute to both of these caustics. In particular, initially they generate the lower part of the fold, they get reflected, and finally they generate the cusp. The trajectory of the transmitted beam is described by Eqs. (31)–(34), whereas the trajectory of the reflected beam is given by Eqs. (31), (32), and (35). Specifically, the upper part of the left branch of the cusp (which satisfies the condition $x < 0$) has a parabolic structure and is given by Eq. (35). The remaining part of the cusp and the lower part of the fold (which satisfy $0 < x < 4$) are given by Eqs. (31) and (32). Finally, the right part of the fold ($x > 4$) is given by Eqs. (33) and (34).

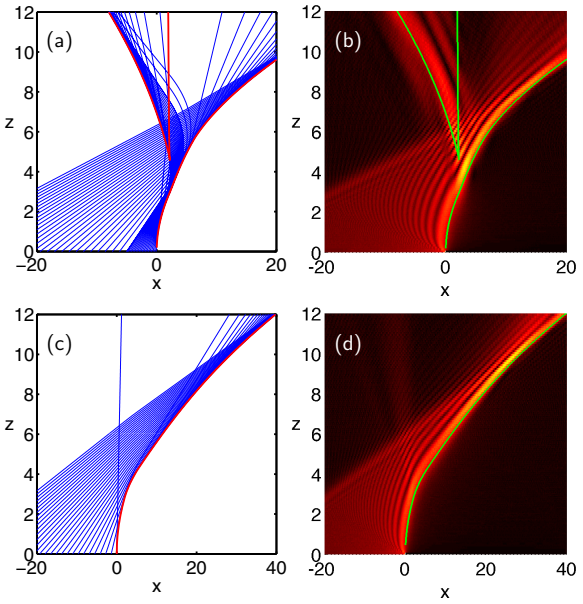

FIG. 2. (Color online) Dynamics of Airy beams propagating in a medium with a piecewise linear sigmoid potential as given by Eq. (12). On the left we see the ray dynamics (blue curves) as well as the caustic trajectories (thick red lines). On the right we see the corresponding direct numerical simulations and the caustic lines in green. In the top row ($\alpha = 2$, $\beta = 2$, $\gamma = 1$, and $x_0 = 4$) the index is decreased from left to right, whereas in the bottom row ($\alpha = -2$, $\beta = 2$, and $x_0 = 4$) the index is increased from left to right.

In Figs. 2(c) and 2(d) $\alpha < 0$ and thus the rays accelerate due to the presence of the potential forming a single transmitted beam.

V. CONCLUSIONS

In conclusion, we have studied the reflection and transmission dynamics of curved Airy beams in the presence of different classes of potentials. These include localized index potentials whose contrast goes to zero outside a bounded region, as well as sigmoid potentials whose index asymptotically takes different constant value outside a bounded region. We studied the general properties of such systems and found analytic expressions for the ray and beam dynamics for particular classes of potentials. We showed that the trajectory and thus the structure of an Airy wave is modified by the potential. An exception is the case of reflection from a medium with a linear index gradient. Our analytical results are in agreement with the numerical simulations.

ACKNOWLEDGMENTS

Supported by the action "ARISTEIA" in the context of the Operational Programme "Education and Lifelong Learning" that is cofunded by the European Social Fund and National Resources and by the Research Project ANEMOS cofinanced by the European Union (European Social Fund—ESF) and Greek national funds through the Operational Program "Education and Lifelong Learning" of the National Strategic Reference Framework (NSRF).

[1] Y. Hu, G. Siviloglou, P. Zhang, N. Efremidis, D. Christodoulides, and Z. Chen, in *Nonlinear Photonics and Novel Optical Phenomena*, Springer Series in Optical Sciences Vol. 170, edited by Z. Chen and R. Morandotti (Springer, New York, 2012), pp. 1–46.
[2] G. A. Siviloglou and D. N. Christodoulides, Opt. Lett. **32**, 979 (2007).
[3] G. A. Siviloglou, J. Broky, A. Dogariu, and D. N. Christodoulides, Phys. Rev. Lett. **99**, 213901 (2007).
[4] M. V. Berry and N. L. Balazs, Am. J. Phys. **47**, 264 (1979).
[5] Y. A. Kravtsov and Y. I. Orlov, *Caustics, Catastrophes and Wave Fields* (Springer, Berlin, 1999).
[6] E. Greenfield, M. Segev, W. Walasik, and O. Raz, Phys. Rev. Lett. **106**, 213902 (2011).
[7] I. Chremmos, N. K. Efremidis, and D. N. Christodoulides, Opt. Lett. **36**, 1890 (2011).
[8] L. Froehly, F. Courvoisier, A. Mathis, M. Jacquot, L. Furfaro, R. Giust, P. A. Lacourt, and J. M. Dudley, Opt. Express **19**, 16455 (2011).
[9] P. Polynkin, M. Kolesik, J. V. Moloney, G. A. Siviloglou, and D. N. Christodoulides, Science **324**, 229 (2009), http://www.sciencemag.org/content/324/5924/229.full.pdf.
[10] J. Baumgartl, M. Mazilu, and K. Dholakia, Nat. Photon. **2**, 675 (2008).
[11] P. Zhang, J. Prakash, Z. Zhang, M. S. Mills, N. K. Efremidis, D. N. Christodoulides, and Z. Chen, Opt. Lett. **36**, 2883 (2011).
[12] A. Mathis, F. Courvoisier, L. Froehly, L. Furfaro, M. Jacquot, P. Lacourt, and J. Dudley, Appl. Phys. Lett. **101** (2012).
[13] A. Salandrino and D. N. Christodoulides, Opt. Lett. **35**, 2082 (2010).
[14] P. Zhang, S. Wang, Y. Liu, X. Yin, C. Lu, Z. Chen, and X. Zhang, Opt. Lett. **36**, 3191 (2011).
[15] A. Minovich, A. E. Klein, N. Janunts, T. Pertsch, D. N. Neshev, and Y. S. Kivshar, Phys. Rev. Lett. **107**, 116802 (2011).
[16] M. A. Bandres, Opt. Lett. **33**, 1678 (2008).
[17] N. K. Efremidis and D. N. Christodoulides, Opt. Lett. **35**, 4045 (2010).
[18] D. G. Papazoglou, N. K. Efremidis, D. N. Christodoulides, and S. Tzortzakis, Opt. Lett. **36**, 1842 (2011).
[19] P. Panagiotopoulos, D. Papazoglou, A. Couairon, and S. Tzortzakis, Nat. Commun. **4**, 2622 (2013).
[20] A. Chong, W. H. Renninger, D. N. Christodoulides, and F. W. Wise, Nat. Photon. **4**, 103 (2010).
[21] I. Kaminer, R. Bekenstein, J. Nemirovsky, and M. Segev, Phys. Rev. Lett. **108**, 163901 (2012).
[22] F. Courvoisier, A. Mathis, L. Froehly, R. Giust, L. Furfaro, P. A. Lacourt, M. Jacquot, and J. M. Dudley, Opt. Lett. **37**, 1736 (2012).
[23] P. Zhang, Y. Hu, D. Cannan, A. Salandrino, T. Li, R. Morandotti, X. Zhang, and Z. Chen, Opt. Lett. **37**, 2820 (2012).
[24] R. El-Ganainy, K. G. Makris, M. A. Miri, D. N. Christodoulides, and Z. Chen, Phys. Rev. A **84**, 023842 (2011).
[25] N. K. Efremidis and I. D. Chremmos, Opt. Lett. **37**, 1277 (2012).

[26] I. D. Chremmos and N. K. Efremidis, Phys. Rev. A **85**, 063830 (2012).
[27] I. Kaminer, J. Nemirovsky, K. G. Makris, and M. Segev, Opt. Express **21**, 8886 (2013).
[28] N. Voloch-Bloch, Y. Lereah, Y. Lilach, A. Gover, and A. Arie, Nature (London) **494**, 331 (2013).
[29] N. K. Efremidis, V. Paltoglou, and W. von Klitzing, Phys. Rev. A **87**, 043637 (2013).
[30] I. Chremmos, G. Fikioris, and N. Efremidis, Antennas Propag., IEEE Trans. **61**, 5048 (2013).
[31] N. K. Efremidis, Opt. Lett. **36**, 3006 (2011).
[32] I. D. Chremmos and N. K. Efremidis, J. Opt. Soc. Am. A **29**, 861 (2012).
[33] P. Chamorro-Posada, J. Sánchez-Curto, A. B. Aceves, and G. S. McDonald, arXiv:1310.1038 [physics.optics].